JYX JYVÄSKYLÄN YLIOPISTO UNIVERSITY OF JYVÄSKYLÄ

This is a self-archived version of an original article. This version may differ from the original in pagination and typographic details.

Author(s): Sippola, Perttu; Perros, Alexander Pyymaki; Ylivaara, Oili M. E.; Ronkainen, Helena; Julin, Jaakko; Liu, Xuwen; Sajavaara, Timo; Etula, Jarkko; Lipsanen, Harri; Puurunen, Riikka L.

Title: Comparison of mechanical properties and composition of magnetron sputter and plasma enhanced atomic layer deposition aluminum nitride films

Year: 2018

Version: Published version

Copyright: © Published by the AVS.

Rights: In Copyright

Rights url: http://rightsstatements.org/page/InC/1.0/?language=en

Please cite the original version:

Sippola, P., Perros, A. P., Ylivaara, O. M. E., Ronkainen, H., Julin, J., Liu, X., Sajavaara, T., Etula, J., Lipsanen, H., & Puurunen, R. L. (2018). Comparison of mechanical properties and composition of magnetron sputter and plasma enhanced atomic layer deposition aluminum nitride films. Journal of Vacuum Science and Technology A, 36(5), Article 051508. https://doi.org/10.1116/1.5038856

Comparison of mechanical properties and composition of magnetron sputter and plasma enhanced atomic layer deposition aluminum nitride films

Perttu Sippola, Alexander Pyymaki Perros, Oili M. E. Ylivaara, Helena Ronkainen, Jaakko Julin, Xuwen Liu, Timo Sajavaara, Jarkko Etula, Harri Lipsanen, and Riikka L. Puurunen

Citation: Journal of Vacuum Science & Technology A **36**, 051508 (2018); doi: 10.1116/1.5038856
View online: https://doi.org/10.1116/1.5038856
View Table of Contents: http://avs.scitation.org/toc/jva/36/5
Published by the American Vacuum Society

HIDEN ANALYTICAL
Instruments for **Advanced Science**
Contact Hiden Analytical for further details:
www.HidenAnalytical.com
info@hiden.co.uk
CLICK TO VIEW our product catalogue

Gas Analysis
- dynamic measurement of reaction gas streams
- catalysis and thermal analysis
- molecular beam studies
- dissolved species probes
- fermentation, environmental and ecological studies

Surface Science
- UHV TPD
- SIMS
- end point detection in ion beam etch
- elemental imaging - surface mapping

Plasma Diagnostics
- plasma source characterization
- etch and deposition process reaction kinetic studies
- analysis of neutral and radical species

Vacuum Analysis
- partial pressure measurement and control of process gases
- reactive sputter process control
- vacuum diagnostics
- vacuum coating process monitoring

CrossMark
click for updates

Comparison of mechanical properties and composition of magnetron sputter and plasma enhanced atomic layer deposition aluminum nitride films

Perttu Sippola,[1,a)] Alexander Pyymaki Perros,[1,2] Oili M. E. Ylivaara,[3] Helena Ronkainen,[3] Jaakko Julin,[4,5] Xuwen Liu,[6] Timo Sajavaara,[4] Jarkko Etula,[7] Harri Lipsanen,[1] and Riikka L. Puurunen[3,6]

[1]*Department of Electronics and Nanoengineering, Aalto University School of Electrical Engineering, P.O. Box 13500, FI-00076 Aalto, Finland*
[2]*Nanovate Oy, Tietotie 3, 02150 Espoo, Finland*
[3]*VTT Technical Research Center of Finland Ltd., P.O. Box 1000, FI-02044 Espoo, Finland*
[4]*Department of Physics, University of Jyväskylä, P.O. Box 35, FI-40014 Jyväskylä, Finland*
[5]*Helmholtz-Zentrum Dresden-Rossendorf, Institute of Ion Beam Physics and Materials Research, Bautzner Landstr. 400, 01328 Dresden, Germany*
[6]*Department of Chemical and Metallurgical Engineering, Aalto University School of Chemical Engineering, P.O. Box 16100, FI-00076 Aalto, Finland*
[7]*Department of Chemistry and Materials Science, Aalto University School of Chemical Engineering, P.O. Box 16100, FI-00076 Aalto, Finland*

(Received 6 May 2018; accepted 6 July 2018; published 30 July 2018)

A comparative study of mechanical properties and elemental and structural composition was made for aluminum nitride thin films deposited with reactive magnetron sputtering and plasma enhanced atomic layer deposition (PEALD). The sputtered films were deposited on Si (100), Mo (110), and Al (111) oriented substrates to study the effect of substrate texture on film properties. For the PEALD trimethylaluminum–ammonia films, the effects of process parameters, such as temperature, bias voltage, and plasma gas (ammonia versus N_2/H_2), on the AlN properties were studied. All the AlN films had a nominal thickness of 100 nm. Time-of-flight elastic recoil detection analysis showed the sputtered films to have lower impurity concentration with an Al/N ratio of 0.95, while the Al/N ratio for the PEALD films was 0.81–0.90. The mass densities were ~3.10 and ~2.70 g/cm^3 for sputtered and PEALD AlN, respectively. The sputtered films were found to have higher degrees of preferential crystallinity, whereas the PEALD films were more polycrystalline as determined by x-ray diffraction. Nanoindentation experiments showed the elastic modulus and hardness to be 250 and 22 GPa, respectively, for sputtered AlN on the (110) substrate, whereas with PEALD AlN, values of 180 and 19 GPa, respectively, were obtained. The sputtered films were under tensile residual stress (61–421 MPa), whereas the PEALD films had a residual stress ranging from tensile to compressive (846 to −47 MPa), and high plasma bias resulted in compressive films. The adhesion of both films was good on Si, although sputtered films showed more inconsistent critical load behavior. Also, the substrate underneath the sputtered AlN did not withstand high wear forces as with the PEALD AlN. The coefficient of friction was determined to be ~0.2 for both AlN types, and their wear characteristics were almost identical. *Published by the AVS.*
https://doi.org/10.1116/1.5038856

I. INTRODUCTION

Aluminum nitride is a direct wide band gap, III–V semiconductor possessing superb dielectric and piezoelectric properties, good thermal conductivity, and mechanical strength. The material is considered an ideal candidate in a diverse array of microelectronic applications, ranging from optoelectronics to microelectromechanical systems (MEMS).[1,2] With each application, different demands are placed on the characteristics of the film: crystalline or amorphous, pure or hydrogen containing, thick or thin, etc. These demands in turn dictate the most appropriate method of deposition. Therefore, AlN has been grown with several deposition methods, such as sputter deposition,[3] metalorganic chemical vapor deposition,[4] molecular beam epitaxy,[5] plasma enhanced chemical vapor deposition,[6] and plasma enhanced atomic layer deposition (PEALD).[7,8] Despite this, there is a lack of systematic comparison between the two main thin film deposition types: physical vapor deposition (PVD) and chemical vapor deposition (CVD) methods of AlN. Specifically, the comparative mechanical performances of the films made with these methods have not attracted much academic attention.

For the PVD methods, magnetron sputter deposition is routinely used to produce films due to the good control of composition, residual stress, and crystalline structure. Consequently, the sputtering process effects on the mechanical properties of coatings have been widely studied.[9–13] Magnetron sputtered AlN has been successfully utilized, for example, on piezoelectric nanoelectromechanical system (NEMS) fabrication,[14] which requires exact stoichiometry, minor residual stress, highly crystalline hexagonal wurtzite structure, and low roughness. Nevertheless, sputtered AlN has been shown to exhibit inhomogeneous microstructure

[a)]Electronic mail: perttu.sippola@aalto.fi

(columnar crystals, several orientations, and pebblelike surface morphology), especially in the beginning of the film growth.[15] Specifically for submicrometer thick sputtered AlN films, one important factor affecting the physical characteristics is the texture of the chosen substrate. The substrate type can also be expected to influence the mechanical properties of the sputtered AlN. An interesting topic is AlN sputtering on oriented metal surfaces. For instance, a highly (002) oriented AlN film sputtered on Mo electrodes has been demonstrated as a viable film bulk acoustic wave resonator, deriving the performance partly from the good acoustic wave propagation properties of the material combination.[16,17]

Despite the many merits of sputtering, the line-of-sight nature of the deposition results in poor conformality which limits its usage mostly on low aspect ratio structures. For these purposes, the modified CVD method called atomic layer deposition (ALD) is an ideal candidate due to its sequential, self-terminating, gas–solid reaction surface growth.[18] This renders ALD its precise thickness control and good conformality[19] and uniformity of the produced film, which make ALD a viable method, for example, for complex NEMS fabrication.[20] However, the thermal ALD of nitrides suffers from poor reactivity of the conventional nitrogen precursors [e.g., ammonia (NH_3)] at typical ALD temperatures (≤500 °C) which has a negative effect on the film quality.[8,21]

In order to overcome the issue of the low reactivity in thermal ALD, PEALD is commonly applied in which the nitrogen precursor is plasma activated.[22] PEALD of AlN has been studied reasonably during the last decade with studies mainly concentrated on the PEALD process parameters' influence on the growth behavior[8,23,24] and the chemical,[7,25] structural,[8,26] optical,[26] and electrical[27] quality of the AlN films. However, important mechanical properties, such as adhesion, friction and wear, hardness, and elastic modulus, have not yet been studied despite their high importance for material reliability in mechanical applications and challenging environments.

Little is known on the comparative mechanical properties of PEALD AlN thin films with respect to more established PVD deposition methods such as sputtering. This is understandable because sputtering is an established method and often its applications require thicker, micrometer range, films and, thus, different mechanical measurement setups are used.[28] Therefore, this research compared mechanical properties of PEALD and magnetron sputter deposited thickness-normalized AlN films with the same methods. The effect of PEALD process temperature, bias voltage, and gas mixture was compared to sputtered AlN films on oriented surfaces of Si, Mo, and Al. To support the mechanical property analysis and quality comparison of the two AlN deposition methods, elemental film composition and x-ray diffraction (XRD)/reflection structural analysis were also conducted.

II. EXPERIMENT

A. Film depositions

Silicon (100) was used as the substrate for the PEALD AlN and sputtered AlN films. The sputtered AlN films were deposited on three different substrates having different crystal orientations: silicon (100), sputtered aluminum (111), and molybdenum (110) seed layers on silicon. These samples are referred to as *S_ref*, *S_Ti/Al*, and *S_Ti/Mo*, respectively. The Al and Mo seed layers had a targeted thickness of 150 nm and were deposited on top of Ti adhesion layers having a nominal thickness of 20 nm. All Si substrates were cleaned with Radio Corporation of America-cleaning sequence (SC-1, HF, SC-2) prior to subsequent deposition.

The PEALD AlN films were deposited with a Beneq TFS-500 ALD reactor in remote plasma mode using a capacitively coupled (CC) radio frequency (RF) plasma source operating at 13.56 MHz. Trimethylaluminum (TMA) (≥98% purity, Sigma-Aldrich) and either NH_3 (5.0 purity, AGA) or N_2/H_2 (7.0 and 5.0 purity, respectively, AGA) were used as precursors for the PEALD of AlN. A plasma power of 80 W was used for all the runs using NH_3, whereas a plasma power of 60 W was used for the N_2/H_2-gas mixture (*PA_N2/H2*) process at 200 °C. The majority of the samples had the CC plasma head under bias voltages of 5–10 V during the plasma pulses. Yet, one 200 °C deposited NH_3 plasma process sample had its bias voltage fixed to 25 V which resulted in a plasma power of 235 W since these parameters are interconnected. This sample is referred to as *PA_25V*.

N_2 carrier gas, NH_3, and the N_2/H_2-gas mixture flow rates were controlled by mass flow controllers while the base pressure was at ∼1 mbar. The flow rates for the N_2/H_2-gas mixture delivered through the showerhead, which also acts as an anode, were 30/120 sccm. The experimental depositions with the NH_3 process were performed at temperatures of 150, 200, and 300 °C, and the corresponding samples are named *PA_150C*, *PA_200C*, and *PA_300C* in this work. The TMA source temperature was kept at 20 °C, pulse time was 400 ms, and purge time was 6 s. For both N_2/H_2 and NH_3, pulse and purge times were 15.75 and 3.25 s with the N_2 source gas introduced in the reactor before plasma ignition. The plasma exposure time was 15 s for all gas mixtures. These precursor doses have been confirmed to be sufficient to ensure the self-termination of the ALD reaction cycles for the setup used in this study.[24] The PEALD process cycle numbers were 1100 for *PA_200C*, 1176 for *PA_150C*, 770 for *PA_300C*, 1000 for *PA_25V*, and 1500 for *PA_N2/H2*, targeting in all cases to 100 nm thickness. In practice, thinner films than targeted were obtained (77–92 nm).

Magnetron sputtered AlN films were deposited with the Tegal AMS-2004 single module sputtering tool (OEM Group). The system uses dual cathode alternating current (AC) S-guns at 40 kHz and, in addition, the sputtering target configuration is equipped with a direct current (DC) power source. No external heating was applied during sputtering; however, the substrate self-heated up to 250 °C due to plasma power flux. In order to obtain optimum AlN growth, the sputtering parameters were chosen specifically for each substrate. For the *S_ref* and *S_Ti/Mo*, the AC power was 4 kW, the DC power was 0.25 kW, and Ar/N_2 flow was 90/35 sccm. In the case of *S_Ti/Al*, the corresponding values were 3, 0.25 kW, and 60/35 sccm. Low power AlN sputtering was applied on the Al seed layer to avoid hillock formation.

As the magnetron sputter is dedicated to AlN thin films, the Ti, Al, and Mo layers were sputtered in a von Ardenne CS 730 S cluster sputtering tool. The tool consists of three chambers for DC, RF, and pulsed-DC sputtering in an ultra-clean environment. The 20 nm Ti for the adhesion layer of the *S_Ti/Al* and *S_Ti/Mo* samples was deposited at 375 °C and with 500 W RF power and 60 sccm Ar flow, with the throttle valve open. The 150 nm Mo was deposited with 1000 W DC power and 66 sccm Ar flow, at room temperature and throttle valve open. In addition, the 150 nm Al was sputtered with 450 W DC power and 60 sccm Ar at room temperature and throttle valve open.

B. Film characterization

An X'Pert Pro Diffractometer with Cu $K_{\alpha 1}$ radiation was used to perform x-ray reflectivity (XRR) measurements for all the films and powder mode ($\theta/2\theta$) XRD measurements for the sputtered films to extract physical properties and structural information. Density, thickness, and surface roughness were obtained by fitting the measured XRR data to a theoretical model using X'Pert reflectivity analysis software. In the case of the PEALD AlN films' crystallinity, surface optimized grazing incidence XRD (GIXRD) scans were measured with a Rigaku SmartLab diffractometer in the parallel beam mode at an incidence angle of 0.4° utilizing a 9 kW rotating anode x-ray source (Cu $K_{\alpha 1}$ radiation) and a 2D detector (HyPix-3000). Despite the two used XRD setups, both were out-of-plane measurements determining crystallographic planes parallel to the substrate surface and therefore the results can be considered comparable.

To study the composition of the AlN films, elemental depth profiling was performed by time-of-flight elastic recoil detection analysis (ToF-ERDA).[29] The PEALD and sputtered AlN films were, respectively, measured using 13.6 MeV ^{63}Cu and 8.5 MeV ^{35}Cl (or 10.2 MeV ^{35}Cl) beams close to mirror geometry.

Residual stress was determined by measuring wafer curvatures before and after the depositions with a TOHO FLX-2320S. The residual stress was determined using Stoney's equation and maximum measurement error as described by Ylivaara *et al.*[30] The film thicknesses on the basis of the stress calculations were determined with XRR. For measurement error estimation,[30] a 3% film thickness nonuniformity was assumed.

The hardness and elastic modulus of the AlN films were studied by the nanoindentation technique using a TriboIndenter® TI-900 (Hysitron, Inc.). A cube-corner shaped indenter with a 90° total induced angle and a nominal tip radius of 40 nm was used in the measurements. A sample measurement included first 25 indents with sequentially increasing indentation depths (5–125 nm) in order to determine dependency between the property and the contact depth. Next, the AlN film was measured from a fresh sample surface area with 25 indents while minimizing the earlier discovered surface and substrate related uncertainties. Still, the extracted film properties had some indentation-to-indentation variations which are presented as error margins averaged from 25 indentations. The high erroneous indent data at shallow depths came mainly from two sources: the surface-related film defects such as roughness and the inaccurate indenter tip area function. The elastic modulus of a film, E_f, was calculated by using the following equation:[31]

$$\frac{1}{E_r} = \frac{1-\nu_i^2}{E_i} + \frac{1-\nu_f^2}{E_f}, \quad (1)$$

where E_i and E_r are the elastic modulus of the diamond tip and the measured reduced/contact modulus, respectively. The ν_i and ν_f are Poisson's ratios of the diamond tip and the AlN film, respectively. For the diamond indenter, $E_i = 1141$ GPa and $\nu_i = 0.07$.[31] The used Poisson ratio of the AlN films was 0.25.[32] The details of the applied hardness analysis are described in Ref. 30.

The adhesion of AlN films was evaluated by scratch testing using a Micro-Combi Tester (Anton Paar TriTec). In the scratch test, a diamond tip (20 μm radius) was used to generate a scratch on the coated surface with progressive loading increasing from 0.05 to 1.3 N. The scratch length was 3 mm and the scratching speed was 10 mm/min. At least three scratches were made for each sample, and the results are presented as average values with standard deviations of the measured values. The experiments were carried out in controlled temperature and humidity (22 ± 1 °C and 50 ± 5% relative humidity). Four critical loads were determined for the coatings:[28] L_{CSi1} indicating the first, local crack generation on the substrate; L_{CSi2} indicating the continuous cracking of the substrate; L_{CAlN1} indicating the first, local delamination of the AlN film; and L_{CAlN2} indicating the continuous delamination of the AlN film.

Tribological measurements to obtain friction and wear characteristics were also carried out using the Micro-Combi Tester (Anton Paar TriTec). The AlN coated Si samples were glued on aluminum discs (Al 6082, diameter 40 mm) to ensure firm fastening to the test device. The counter surface was a hemispherical silicon pin with a 50 mm radius of curvature polished to mirror finish and cleaned before testing with petroleum ether, ethanol, and acetone. A constant load of 300 mN was used during the tests with a sliding speed of 0.01 ms^{-1} and a length of the sliding pass of 10 mm in one direction. The testing was carried out in a stepwise manner with 50, 100, 200, 300, and 500 sliding passes for each test. After each step, the friction coefficient was determined as the mean value of one sliding cycle, and the condition of the coating was investigated by optical microscopy. The sliding distance of 500 passes generated in total the sliding distance of 5 m. After the tests, the contact surfaces were studied, and the wear of the silicon pin was determined by determining the worn area by microscopy.

III. RESULTS AND DISCUSSION

A. Thickness, density, and roughness

The thickness, density, and roughness of AlN films determined x-ray reflectivity analysis are presented in Table I.

TABLE I. XRR analysis, residual stress, hardness, and elastic modulus results of PEALD and sputtered AlN. The simulated densities have an accuracy of ±0.05–0.1 g/cm^3 and the thicknesses ±0.2–0.5 nm (Ref. 30). The error in residual stress is approximated using the total differential method as presented in Ref. 33. In the hardness and elastic modulus figures, the error is based on average variation of 25 indentations for each sample.

Sample	Thickness (nm)	GPC (Å/cycle)	Density (g/cm^3)	Roughness (nm)	Residual stress (MPa)[a]	Hardness (GPa)	Elastic modulus (GPa)
S_ref	90.7	—	3.25	2.0	61 ± 10	—	—
S_Ti/Mo	88.9	—	3.15	2.0	101 ± 14	22.3 ± 0.9	250 ± 27
S_Ti/Al	101	—	2.85	2.2	421 ± 31	—	—
PA_300C	90	1.17	2.76	1.6	846 ± 53	19.6 ± 0.7	175 ± 4
PA_200C	90.5	0.82	2.7	1.6	220 ± 18	16.9 ± 0.4	157 ± 4
PA_150C	92	0.78	2.63	1.6	175 ± 20	15.2 ± 0.5	160 ± 10
PA_25V[b]	84.0	0.84	2.90	2.5	−47 ± 9	19.1 ± 1.0	180 ± 10
PA_N2/H2[b]	76.8	0.51	2.46	1.0	450 ± 34	14.0 ± 0.3	155 ± 6

[a]The positive value indicates tensile stress and the "—" sign compressive.
[b]These samples were deposited at 200 °C.

In addition, the growth-per-cycle (GPC) of the PEALD processes is shown as they reveal more about the growth behavior. A comparison of PEALD and sputtered AlN samples shows that significantly higher densities are obtained for the sputtered films. The measured density of 3.25 g/cm^3 for the *S_ref* is the same as reported for the fully crystalline AlN.[33] On the contrary, the PEALD samples had density values close to values reported for amorphous or polycrystalline PEALD AlN films (2.5–2.8 g/cm^3).[7,24,25] The nanoscale roughness results showed PEALD films to be slightly smoother compared to sputtered films. The slightly higher average roughness of the sputtered films could be attributed to the crystalline or polycrystalline structure of the film (see Sec. III C).[3,11]

The densities of sputtered AlN films were the highest on the (100) Si substrate, while on the Al substrate, the sample *S_Ti/Al*, AlN had a density of 2.85 g/cm^3 which compares to the PEALD film having the highest density, 2.90 g/cm^3. The sample *S_Ti/Mo* showed a density of 3.15 g/cm^3. These results show that the chosen substrate has a significant effect on the density of the sputtered AlN, while the nanoscale roughness remained practically constant (∼2.0 nm) indicating thus the similar size of surface crystallites. It should be noted that the simulated XRR values of sputtered AlN have slightly larger uncertainties than PEALD films due to poor initial growth quality.[15] In addition, the layer structure analysis of the *S_Ti/Al* showed that the Al and Ti interlayer structure was defective. ToF-ERDA compositional depth determination supported the interpreted defectiveness by showing increased elemental impurities (Ti, N, and O) in the Al interlayer and its interfaces. Therefore, the relatively low density of the *S_Ti/Al* is likely a result of this structurally and chemically unfavorable texture for AlN sputtering.

In the case of the PEALD AlN, density and GPC increase as a function of the deposition temperature: between 150 and 300 °C the density increased from 2.63 to 2.76 g/cm^3 and GPC from 0.78 to 1.17 Å/cycle. These results are in-line with the same temperature range TMA/NH_3 process results of Bosund *et al.*[24] The increasing GPC and density can be attributed to higher thermal energy causing increased reactivity of precursors which resulted in more complete bonding reactions. It is also possible that the thermal NH_3 had a minor deposition component during the plasma half cycle of the process. Interestingly, the *PA_25V* sample shows high density (2.90 g/cm^3), but not increased GPC in comparison to the lower bias voltage AlN of the *PA_200C*. Therefore, the higher plasma bias voltage on the *PA_25V* primarily leads to densification of the film structure with respect to the lower bias process (2.90 vs 2.70 g/cm^3) and likely results in a higher degree of the polycrystalline structure of AlN judging also from the higher level of roughness (2.5 vs 1.6 nm). The conclusion can be made that increased bias voltage is an alternative to raising the deposition temperature for improving some material properties.

The sample *PA_N2/H2* had a GPC of 0.51 Å/cycle, which is less than that reported for otherwise similar but for a 80 W plasma power process by Pyymaki Perros *et al.*[25] (0.61 Å/cycle) which also has a higher reported density. The cited study also suggested that the insufficient reactions reduce the GPC of the TMA and N_2/H_2 capacitively coupled plasma processes. Yet, for the same precursor combination using inductive coupled plasma (ICP) based ALD processes, the GPC of 1 Å/cycle has been reported by Goerke *et al.*[34] The previous research also showed that improper process conditions resulted in an increase of GPC as a form of post-ALD surface oxidation.[34] A likely reason for the relatively low GPC was the combination of the low plasma power (60 W) resulting in low reactivity of the N_2/H_2 and the PEALD reactor specific growth.

B. Elemental composition

The elemental composition (at. %) of the AlN samples as obtained by ToF-ERDA is presented in Table II. These values for the films were determined from the depth profiles (Fig. 1) omitting the surface and interface regions. The analysis shows sputtered AlN films to have a more preferable stoichiometry (an Al/N ratio close to 1) and less impurities than in the PEALD films. The most notable difference is the high H concentration found in the PEALD films which has been noted also in earlier studies at similar process

TABLE II. ToF-ERDA determined elemental compositions of the AlN films with omited surface and interface impurities.

Sample	Al (at. %)	N (at. %)	O (at. %)	C (at. %)	H (at. %)	Cl (at. %)	Ar (at. %)	Al/N
S_ref	48.4 ± 0.7	51.0 ± 0.7	<0.15	<0.15	<0.3	—	<0.05	0.95
S_Ti/Mo	49.2 ± 0.6	50.5 ± 0.8	<0.2	<0.15	<0.1	—	—	0.97
S_Ti/Al	48.6 ± 0.4	50.9 ± 0.4	<0.15	<0.1	<0.1	—	<0.3	0.95
PA_300C	39.0 ± 1.0	44.0 ± 1.0	0.4 ± 0.1	1.6 ± 0.2	14.2 ± 0.5	0.7 ± 0.1	—	0.89
PA_200C	37.2 ± 1.0	43.9 ± 1.0	0.2 ± 0.1	0.7 ± 0.1	16.9 ± 0.5	1.2 ± 0.1	—	0.85
PA_150C	34.5 ± 1.0	42.7 ± 1.0	0.3 ± 0.1	0.6 ± 0.1	20.4 ± 0.5	1.5 ± 0.2	—	0.81
PA_25V	41.2 ± 1.0	45.9 ± 1.0	0.2 ± 0.1	0.35 ± 0.1	11.8 ± 0.5	0.6 ± 0.1	—	0.90
PA_N2/H2	33.6 ± 1.0	40.0 ± 1.0	0.3 ± 0.1	2.5 ± 0.2	21.5 ± 1.0	2.2 ± 0.2	—	0.84

temperatures.[24,25] Also, both films are N-rich, but the PEALD AlN films have a significantly lower Al/N ratio (∼0.85) than the sputtered AlN (0.95).

The PEALD AlN films contained significant concentrations of H, showing a reduction from 20.4 to 14.2 at. % with increasing deposition temperatures from 150 to 300 °C. Similar inverse correlation of H concentration regarding the deposition temperature has also been shown for AlN in an earlier study.[24] All of the used precursors (TMA, NH_3, and N_2/H_2) can be the source of H, and thus H could be expected to exist in the molecular form as a part of -CH_x and -NH_x groups. The *PA_300C* sample contained more C than the other NH_3 based PEALD samples, which could result from a slight decomposition of TMA. The C impurity concentrations (0.35–2.5 at. %) of the PEALD AlN films represent a good average in comparison to other TMA based PEALD of AlN studies in which the C concentrations range from 0.39 to 4.2 at. %.[7,25]

It is interesting to note that the AlN deposited under higher bias, the *PA_25V*, contained less H and other impurities, excluding oxygen, than the other PEALD films. This could be attributed to the high-bias effect which caused enhanced ion energies and possibly enhanced radical doses to the substrate. Suitable ion energies and fluxes have been shown to enhance ligand-removal and adatom migration, and thus increasing the number of available surface sites and facilitating their saturation.[35] This could have led to a decrease of precursor based (C and H) impurities and improved the stoichiometry. The films were almost free of O with a rather constant level of O (∼0.3 at. %), which could be attributed to a small background presence of H_2O inside the reactor. The ERDA procedure used here is known to exaggerate the O content in the film bulk in the presence of strong surface and interface O peaks, since effects such as multiple scattering are not taken into account in this type of analysis. Similar to O, the source of Cl impurities can be credited to a systematic background contamination caused by a shared metallic precursor line of halides and TMA. In addition, an influence of TMA (98%) containing trace amounts of Cl could have also caused minor chlorination of the films. Only the high-temperature and high-bias processes seem to reduce the Cl incorporation to the films. Similar background Cl impurities have been observed in AlN using the same tool.[25]

In the case of the N_2/H_2 precursor based process, the C, H, and Cl impurity concentrations are the highest, which indicates that the surface reactions with 30/120 sccm N_2/H_2 were not as efficient as those with the NH_3 process. In the earlier research of Pyymaki Perros *et al.*,[25] the same PEALD N_2/H_2 process, differing only by 80 W plasma power, yielded a similar magnitude Al/N ratio of 0.88 as our process (0.84). The slight difference could be attributed to the low plasma power of 60 W, which likely resulted in insufficient NH_x and CH_x surface species removal.

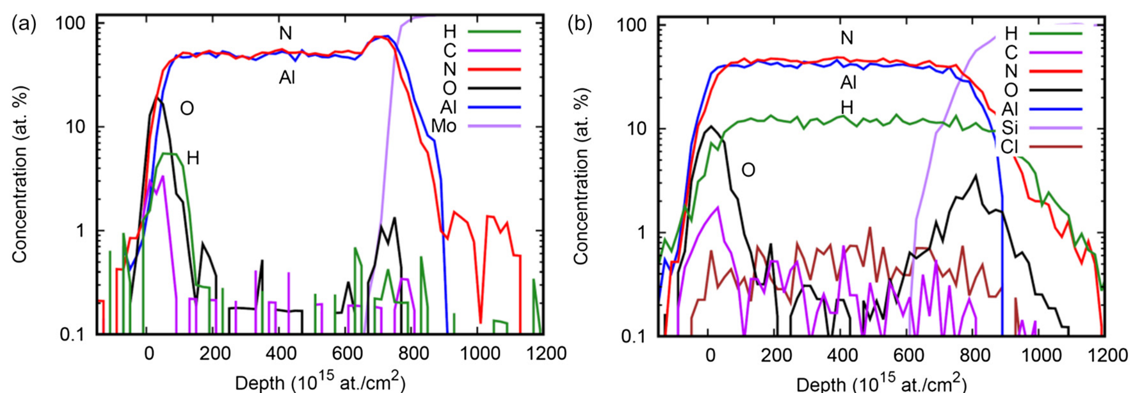

FIG. 1. ToF-ERDA depth profiles of AlN deposited with (a) sputtering on the Ti/Mo substrate and (b) 25 V bias PEALD. The elevated Al and N levels on the Mo interface are an artifact of the analysis process due to higher stopping force of Mo.

In contrast to the PEALD films, the sputtered AlN films contain only low amounts of H, O, C, and Ar in the bulk of the films, hence only the upper atomic concentration limits could be given. The stoichiometry (~0.95) and impurity levels of the AlN films sputtered on three different substrates do not have significant differences. Some samples showed trace amounts, near the detection limit, of Ar at the interface of sputtered AlN which originate from the carrier gas of the sputter system.

Figure 1 presents exemplary logarithmic ToF-ERDA depth profiles from the PEALD and sputtered AlN films of the samples *PA_25V* and *S_Ti/Mo*, respectively. Both PEALD and sputtered films have a pronounced surface. The C and H impurity levels peak at the surface of the sputtered and PEALD films. The surface oxidation and impurity formation can be attributed to postdeposition ambient air exposure.

C. Crystallinity

The AlN films were measured with XRD to study roughly the comparative degree of crystallinity. The PEALD AlN films were originally measured under a similar powder mode XRD setup as used for the sputtered films but no crystallinity could be found. Therefore, the PEALD AlN films were remeasured with a more surface optimized GIXRD setup. Usually a distinct (002) preferential orientation (i.e., the *c*-axis perpendicular to the substrate surface) of AlN is considered as the most valuable crystallographic quality factor, especially for piezoelectric applications. Figures 2 and 3 illustrate the diffractograms of the sputtered and PEALD AlN films, respectively. The full-width-at-half-maximum (FWHM) peak center positions at 36.05° for the sputtered and PEALD AlN were in good agreement with the database peak position of 36.04° for the hexagonal (002) peak[36] (based on the inorganic crystal structure database (ICDS) value).

The *S_Ti/Al* had two dominating diffraction peaks indicating (002) and (101) (at 38.65°)[37–39] orientated crystalline AlN. Since the (101)/(002) ratio is clearly larger than one, it seems that the growth on this Al surface favors the (101) orientation instead of the (002). Moreover, the moderate intensity peak at 33° has traditionally contributed to the (100) orientation of AlN deposited by sputtering.[9,38,39] In our case, however, it is more likely that it is from Si(200) reflection because the peak is narrower than the AlN peaks. Furthermore, Liu *et al.*[12] reached a similar conclusion.

In earlier magnetron sputtered AlN film crystallography studies, (100) and (101) preferential growth has been obtained with certain operational pressure,[37] N_2 concentration,[38] process temperature,[39] and RF power[39] values. Therefore, the potential (101) orientation favoring the influence of the process parameters to the *S_Ti/Al* cannot be ruled out because the other sputtered AlN films were done with a slightly different sputtering process and their XRD results do not show the (101) orientation peaks. Thus, the (101) orientation crystallites can be seen as a result of the poor quality seed layer material (as suggested by the XRR results) and/or unoptimized sputtering process parameters. Moreover, the *S_ref* showed practically strong (002), (004), and (100) preferential orientations than the *S_Ti/Al*, correspondingly. The intensity of the (004) peak indicates only an insignificant randomness of crystalline orientations.

It is noteworthy that the AlN thickness of the XRD measured *S_Ti/Mo* sample was 300 nm and not 100 nm as is the thickness of the rest of the samples in this work and, therefore, its AlN peak [(002) and (004)] intensities are higher.[40] Besides the AlN peaks, this sample shows a (110) orientation Mo peak at 40.7°, which is characteristic to sputtered AlN/Mo bilayer films.[16,17,41] The overall crystallographic quality of the *S_Ti/Mo* was good considering the existing mismatch with the (110) oriented Mo lattice and the (002) oriented AlN growth. The results would suggest that the mismatching crystal orientation of the substrate does not have high significance on the sputtering of highly (002) oriented AlN. This interpretation is also supported by earlier research.[16]

The PEALD AlN films were found to be polycrystalline with dominantly (100), (002), and (101) orientated crystallinity, whereas other AlN orientations [such as (110) and (103)]

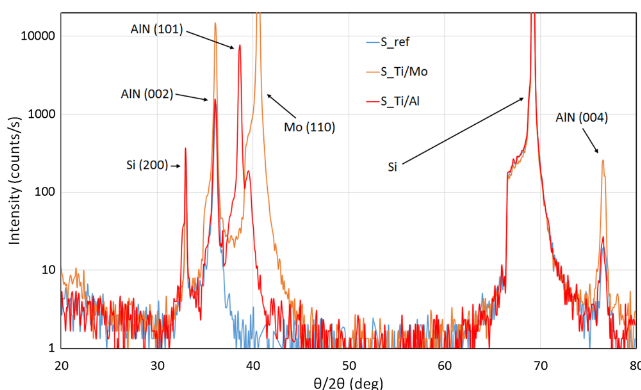

Fig. 2. XRD $\theta/2\theta$ scans obtained from AlN films deposited with sputtering (*S_ref*, *S_Ti/Mo*, and *S_Ti/Al*). The *S_Ti/Mo* sample had an AlN thickness of ~300 nm while the others had ~100 nm thickness. Also, *S_Ti/Al* had a defective Ti/Al material layer underneath the AlN. This likely effected the preferential growth.

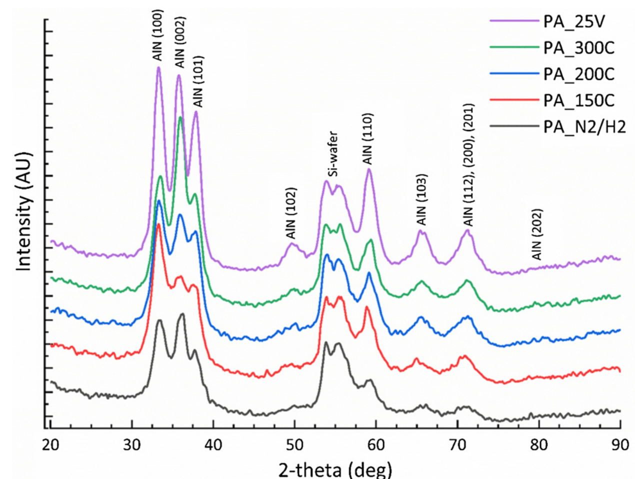

Fig. 3. As-measured GIXRD patterns with constant offset of the PEALD AlN samples at 0.4° incidence angle and with AlN planes indexed.

showed lesser prevalence, as can be seen from Fig. 3. Also, their average crystallite size, as estimated by the Scherrer method using the (100) reflection, was found to vary roughly from 4 to 6 nm (see the supplementary material[46] for more information). Similar XRD results have been shown earlier for PEALD AlN having varying degrees of polycrystallinity.[24,34,42] As estimated from the relative intensities of diffraction peaks in Fig. 3, a higher degree of crystallinity and preferred (002) orientation correlate with increased deposition temperature. Furthermore, since the (100) orientation has been reported as the most intensive peak in powder AlN diffractograms,[43] it can be seen that at least the *PA_300C* AlN has a preferential (002) orientation crystallinity while the lower temperature processes favor this to a lesser extent. Interestingly, the *PA_25V* film GIXRD peak data suggested a high degree of crystallinity and a highly multioriented structure. Since also the *PA_200C* (deposited with about 10 V bias voltage) showed similar relative peak patterns, it seems that plasma bias control does not impart control over any single preferential crystal orientation AlN. From the PEALD samples, the *PA_N2/H2* showed the lowest relative level of overall indicated crystallinity likely due to the influence of the low plasma power process. The presented GIXRD results are also supported by the density, roughness, and Al/N ratio results which were higher for films showing the lowest FWHM thus indicating a higher degree of crystallinity (especially the *PA_25V* and the *PA_300C*). In previous PEALD AlN studies, the degree of crystallinity has been shown to extend from amorphous[7,24] to polycrystalline[8,26] and even to the epitaxial grade [the (002) rocking curve being 144 arcsec][44] depending on the process parameters, chosen substrate, surface treatment, and PEALD reactor setup. These aspects affect the impurity levels which in turn are known to affect crystallinity.

D. Residual stress

The biaxial residual stress results for the sputtered and PEALD AlN films are presented in Table I. The positive stress figures stand for tensile stress and negative figures for compressive stress. Both sputtered and PEALD films show a moderate level of residual stress. Low intrinsic film stress is considered paramount for many device applications, such as piezoelectric actuators or membranes, and are known to promote reliability (less cracking, bowing, blisters, etc.).

The sputtered AlN films were under tensile residual stress (61–421 MPa), where the *S_ref* film was under low 61 MPa stress. In earlier research of sputtered AlN on (100) Si, a good control of stress with sputtering N_2 concentration, pressure, and power has been demonstrated.[12] This general advantage of the established film property control of sputtering has thus been successfully shown. The AlN samples with seed layers show also moderate stresses although the *S_Ti/Al* film has clearly the highest stress from the sputtered samples. The sputtered seed layers of Ti/Mo (47 MPa) and Ti/Al (−75 MPa) also showed low stress. In comparison, a previous study of sputtered AlN on Al (100 nm/100 nm) and the Si substrate has shown the film to have −840 MPa stress, while the 100 nm of AlN on Si produced a stress of −340 MPa.[13] The reason why the cited stress results are compressive while ours are tensile can be attributed to the suitably selected sputtering process parameters. Besides the process parameters, the work of Lee *et al.*[13] also showed residual stress of AlN to change from tensile (450 MPa) to compressive (−630 MPa) with increasing film thickness (10–200 nm).

In the case of the PEALD AlN films, the obtained stress range was larger extending from tensile (846 MPa) to slightly compressive (−47 MPa). Interestingly, our results demonstrate stress level control achieved with the control of the bias voltage of the CCP reactor operated in remote mode during NH_3 plasma: bias voltage of ∼10 V induced a 220 MPa tensile stress while 25 V induced a −47 MPa compressive stress. Similarly, Rontu *et al.*[8] have showed remote ICP based PEALD AlN film stress tuning to be possible from tensile to highly compressive by altering the plasma time of the $AlCl_3/NH_3$ process. In addition, Goerke *et al.*[34] showed minor ICP power dependency to film stress with the TMA/N_2:H_2 PEALD process at 150 °C. In that research, a 300–150 W plasma power produced 390–320 MPa tensile stresses, respectively, and the 150 W films were shown to be suitable for AlN membrane fabrication.[34] These results suggest that the plasma parameter control has a major influence on the stress determination of the AlN film, and thus the PEALD can be considered to be comparable to sputtering on their film stress control capability. It is suggested that sufficiently energetic ion fluxes on the substrate would promote stress formation.[35] However, the earlier studies[30,35] concern mainly oxygen plasma effects on stresses of metal oxide films and therefore more research is needed to obtain more fundamental understanding on the stress formation of the PEALD AlN.

The PEALD temperature is found to affect the residual stress. However, the viable control range is more limited than with the plasma bias voltage: the deposition temperature variation between 150 and 300 °C yielded tensile film stresses of 175–846 MPa. Therefore, the practical freedom of temperature based stress control seems to be limited within the domain of tensile stress. The reason for the dependence of tensile stress and deposition temperature could be related to the crystallinity of the films. It is possible that the multiorientation crystallinity in lower deposition temperature films reduced tensile stress in comparison to the preferentially (002) oriented, 300 °C deposited AlN. Similarly, also the magnitudes of the impurity concentrations influenced the stresses by introducing disorder in the structure and affecting the grain distributions in the films. It is noteworthy that the difference between the coefficients of thermal expansion of the preferentially (002) oriented AlN (5.3×10^{-6} K^{-1})[1] and Si (3.6×10^{-6} K^{-1})[1] is relatively minor, thus their difference can be ruled out as a significant source to stress formation.

The PEALD with N_2/H_2 plasma gas and 60 W yielded higher stress (450 MPa) compared to the *PA_200C* reference sample (220 MPa). The low plasma power results in low ion energies to the substrate which in turn cause low level of crystallinity, less densely packaged film, and more tensile

stress. Also, as shown by the above ToF-ERDA results, the *PA_N2/H2* had also increased atomic impurities of relatively large atoms (2.5 at. % of C and 2.2 at. % of Cl) than the other samples, and thus these could play a role on the increased stress. When considering the above presented temperature effect to stress, the obtained stress result is adequately in-line with the results of Goerke *et al.*[34] who obtained 320 MPa tensile stresses for their N_2/H_2 plasma based AlN at 150 °C.

E. Nanomechanical properties

Hardness and elastic modulus were measured with nanoindentation from all of the PEALD AlN films and from the *S_Ti/Mo* of the sputtered films. The results are presented in Table I. Both the elastic modulus and hardness were higher for the sputtered AlN film on Ti/Mo than for the PEALD films.

In earlier studies, it has been reported that reactive magnetron sputtered AlN on (100) Si can reach hardness and elastic modulus levels of 10–21 and 123–201 GPa, respectively, depending on the sputtering pressure.[9] In the case of helicon sputtered, epitaxial grade AlN (400 nm thick) on a GaN substrate, hardness of 22 GPa and an elastic modulus value of 332 GPa have been obtained.[32] The cited results suggest that the *S_Ti/Mo* outperforms typically reported reactive magnetron sputtered AlN and exhibits similar hardness (22 GPa) than the helicon sputtered epitaxial AlN while the elastic modulus (250 GPa) is still significantly high for magnetron sputtered AlN. The high nanomechanical performance could be contributed to suitably optimized sputtering parameters and a possible favorable effect of the Ti/Mo bilayer. Also, the degree of crystallinity and the crystalline orientation of AlN can be seen to play a major role on the nanomechanical properties of the films because different lattice planes in the hexagonal lattice have differing mechanical properties (i.e., anisotropy of the property). Consequently, it is interesting to note that according to our results, the minor presence of (004) oriented AlN has not reduced the hardness in comparison to epitaxial AlN.[32] Similar conclusion can be made on the sputtered AlN XRD and nanoindentation results of Wei *et al.*[9] These results would suggest that also slightly non-(002) oriented AlN could produce high degree of hardness. It should be noted that in the nanoindentation analysis, the substrate effect on the measured properties was minimized but it was impossible to eliminate it altogether especially for hard coating–soft substrate combinations. Moreover, the substrate effect was more pronounced on the elastic modulus determination because the plastic zone (affects hardness) under the tip was much smaller than the elastic zone (affects elasticity).

The nanomechanical performance of the PEALD AlN films correlates roughly with the density, the degree of crystallinity, and the impurity levels: the low-temperature and N_2/H_2 deposited films have relatively low elastic modulus and hardness (∼160 and ∼15 GPa, respectively), while the high-temperature and high-bias films have higher values (∼180 and ∼19.5 GPa, respectively). These correlations can also be explained with the previously mentioned connection between the degree of crystallinity and the nanomechanical properties since higher degree of crystallinity provides higher hardness and elastic modulus. Thus, the temperature and the plasma parameters influence the nanomechanical properties of the PEALD AlN. Also, the elastic modulus and hardness values of PEALD TiN (186 and 19 GPa, respectively) has been studied to have similar values than the sample *PA_25V*.[45] In the case of the mechanical properties of ALD materials in general, oxides have been more studied. In comparison, the PEALD AlN film shows higher corresponding values than reported for hardness (∼10 GPa) and elastic modulus (∼160 to 170 GPa) of ALD Al_2O_3 films.[30]

F. Adhesion

The scratch tests on the uncoated (100) Si substrate reference yielded critical load results of L_{CSi1} 430 ± 29 mN and L_{CSi2} 668 ± 13 mN. Higher critical load values (than the Si ones) received from coated samples would indicate that the films improve the load carrying capacity and protect the substrate from failure as has been shown for ALD Al_2O_3 on Si wafer.[28] For the PEALD and sputtered AlN films, this feature was not observed. However, the critical values L_{CSi1} and L_{CSi2} for PEALD films were mostly on the similar level compared to uncoated Si as shown in Fig. 4. Only the *PA_N2/H2* provided higher critical load values for silicon failure compared to the uncoated case. It was also typical for the PEALD films that the first crack generation on the Si substrate (L_{CSi1}) led to continuous cracking failure of silicon (L_{CSi2}). The only exception ($L_{CSi1} < L_{CSi2}$) was the *PA_25V* film that showed individual cracks with lower load compared to the other PEALD films. This might be an effect of the high degree of polycrystallinity and compressive stress since the *PA_25V* was the only sample exhibiting these properties.

The critical loads for the continuous delamination of the PEALD AlN films were high, but some local delamination occurred with lower loads as shown in Fig. 4. For the coatings *PA_150C*, *PA_25V*, and *PA_N2/H2*, the first local delamination of the coating (L_{CAlN1}) occurred simultaneously with the continuous fracture of the Si substrate (L_{CSi2}). Interestingly, comparison of the *PA_150C* and *PA_N2/H2* to the *PA_25V* shows that the higher impurity level, more amorphous structure, and lower density do not seem to have a major effect on adhesion. The best adhesion of the PEALD deposited AlN films was measured for the *PA_300C* coating. Despite the variations between the measured critical load values, it could be that the more preferentially (002) oriented crystallinity of the 300 °C deposited film improves the adhesion since also the *S_ref* exhibits the same property combination.

The sputtered AlN films had large variation in all critical load values. The best adhesion performance in terms of AlN film delamination for both critical loads, L_{CAlN1} and L_{CAlN2}, was measured for the *S_ref* sample. For this coating, the critical loads for coating cracking and delamination were even higher than the critical loads of the *PA_300C* film. The sputtered AlN films with seed layers, the *S_Ti/Mo* and *S_Ti/Al*, had lower critical load values. The samples had low L_{CSi1}

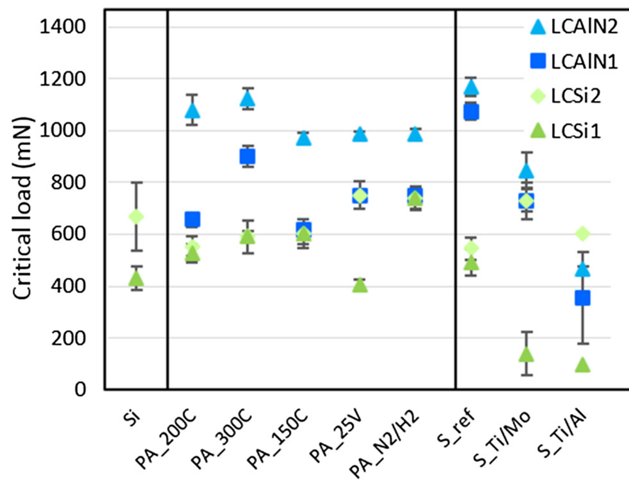

FIG. 4. Critical load values in microscratch testing for the uncoated silicon (Si), ALD films, and sputter deposited films. L_{CSi1} refers to the first observed crack in the Si substrate, L_{CSi2} refers to the beginning of the continuous cracking of the Si substrate, L_{CAlN1} is the first observed local delamination of the coating, and L_{CAlN2} is the continuous delamination of the coating.

values representing local crack generation on Si with minor load. The L_{CSi2} values were on a similar level to uncoated Si. The critical load for continuous coating delamination was lower for both the coatings compared to the PEALD AlN films, thus indicating Ti/Mo and Ti/Al interlayers' negative effect on sputtered AlN adhesion. Particularly, the *S_Ti/Al* coating suffered delamination even before the cracking of silicon providing low L_{CAlN1} and L_{CAlN2} values.

G. Tribological properties

The tribological properties were determined for the sputtered (*S_Ti/Mo*) and PEALD (*PA_200C*) AlN films. Figure 5 presents the coefficient of friction (CoF) values as a function of the sliding contact cycles during which the Si pin was sliding against the coated samples. The friction is about 0.2 for both the coatings in the beginning of the test. The friction of the *PA_200C* film increased and after 100 sliding cycles reached values around 0.63. As the test continues, the CoF stabilized to 0.6. The contact area of the *PA_200C* film was covered by silicon transferred from the silicon pin, forming a tribolayer on the coating surface. Due to this tribolayer formation, sliding occurred between similar surfaces thus increasing friction. Similar friction performance has been previously observed for, e.g., ALD Al_2O_3 films.[45] Both the tribolayer formation on the *PA_200C* film and wear of the silicon pin can be clearly seen in Fig. 6 which represents the contact surfaces after the tests.

The sputtered *S_Ti/Mo* film started to peel off from the substrate surface quite early in the test. Toward the end of the test, the coating was peeled off from the complete contact area. The coating removal increased the friction, and the CoF was in the range 0.66–0.8 during the test as observed in Fig. 5. In Fig. 6, the complete removal of the *S_Ti/Mo* coating can be observed. The removal of the coating suggests insufficient adhesion of the coating for

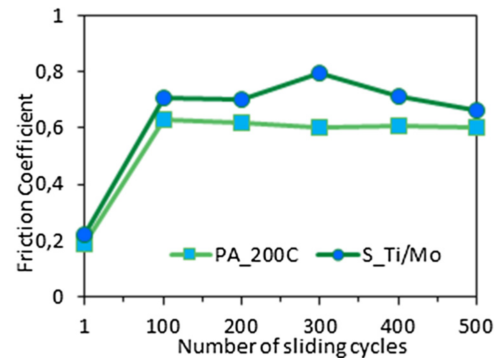

FIG. 5. Friction coefficient of the PEALD *PA_200C* film and the sputtered *S_Ti/Mo* film in reciprocative tests sliding against the silicon pin. The normal load of 300 mN, the sliding speed of 0.01 ms^{-1}, and 10 mm sliding pass in one direction were used in the tests.

these sliding tests. In scratch testing, the critical load value, L_{CAlN2}, for the *S_Ti/Mo* was also lower compared to the *PA_200C*. In Fig. 6, the higher wear of the silicon pin sliding against the *S_Ti/Mo* [1800×10^{-6} $mm^3(N\,m)^{-1}$] compared to the *PA_200C* [790×10^{-6} $mm^3(N\,m)^{-1}$] can be observed.

As a comparison to friction performance of other ALD nitrides, the PEALD and sputtered AlN coatings showed lower friction compared to TiN (CoF ranging from 0.24 to 0.78), but higher friction compared to NbN (CoF in the range of 0.2–0.36).[45]

IV. SUMMARY AND CONCLUSIONS

PEALD and reactively magnetron sputtered AlN films were compared with respect to their mechanical properties, such as residual stress, hardness, elastic modulus, adhesion, and wear. In addition, to support the comparison, elemental, structural, and crystallinity composition analyses were made. The effect of temperature, plasma nitrogen-source gas, and plasma bias voltage to the PEALD AlN films and the effect of Si substrate and sputtered interlayers of Ti/Mo and Ti/Al to sputtered AlN were studied.

All AlN films were on the order of 100 nm thick. The sputtered films had higher mass densities than PEALD AlN ($\leq$3.25 vs $\leq$2.9 g/cm^3, respectively). The elemental impurities of sputtered AlN were at a low level and the Al/N ratios were 0.95–0.97, whereas for the PEALD AlN, Al/N ratios were 0.81–0.90. The PEALD AlN included typical impurities such as H (11.4–21 at. %), C (<0.5 at. %), and O (<0.5 at. %). The sputtered AlN films on Si and Mo were found to have preferentially (002) orientation crystallinity, while the PEALD AlN films had varying degrees of polycrystallinity according to XRD.

The PEALD AlN film stress was found to be controllable with plasma bias voltage from tensile to compressive (220 to −47 MPa), while the deposition temperature showed control of tensile region stress (175–846 MPa). The sputtered films had low to moderate tensile stresses (61–421 MPa), and the interlayer lattice mismatch had no marked effect on the

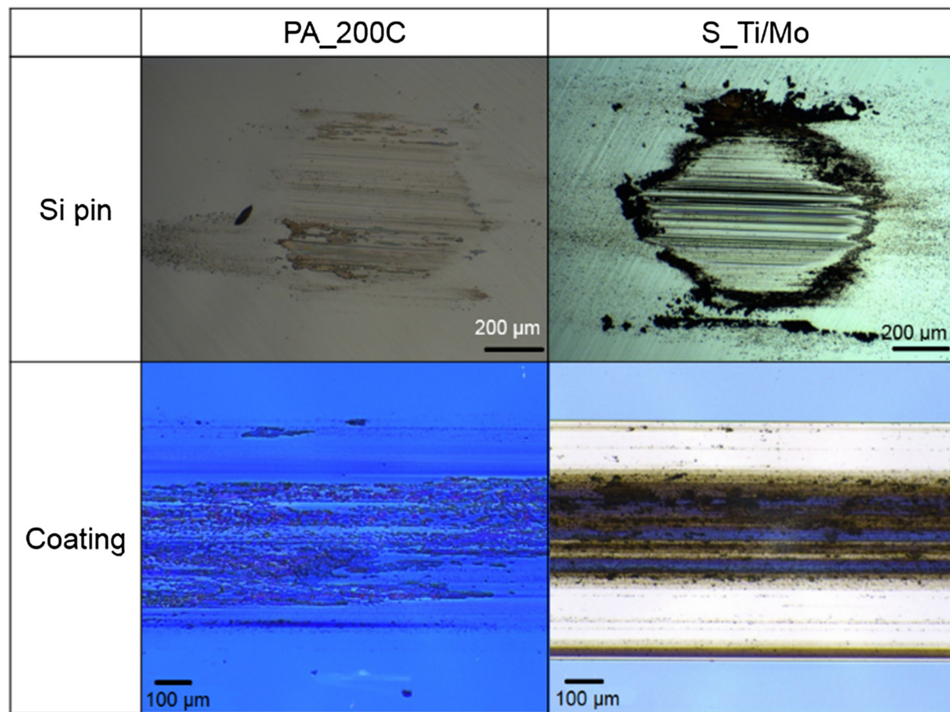

FIG. 6. Contact surface of the PEALD *PA_200C* film, the sputtered *S_Ti/Mo* film, and the Si pins slided against the coated samples.

stress. The nanomechanical analysis revealed elastic modulus and hardness to be high for sputtered AlN on Ti/Mo (250 and 22 GPa, respectively) and lower for the PEALD AlN films (up to 183 and 19 GPa, respectively). The high-temperature PEALD and the sputtered AlN films on Si showed best adhesion performance, but generally the films were not able to protect the Si substrate underneath from cracking. In addition, the adhesion of the PEALD films behaved in a more consistent fashion than the sputtered films. The tribological properties were similar for both types of films having an initial coefficient of friction of 0.2 with an increasing trend, reaching values in the range of 0.6–0.7 in a prolonged test. On the PEALD AlN film, a transfer layer of silicon was formed on the sliding surface, which is typically observed to increase friction. For the sputtered AlN on Mo/Ti, the complete removal of the coating occurred revealing the silicon substrate surface.

To conclude, the sputtered AlN showed precise stoichiometry and crystallinity, which resulted in high structural quality, elastic modulus, and hardness in comparison to the more nonstoichiometric PEALD AlN. Yet, the adhesion and wear properties of the AlN films did not seem to be clearly sensitive to the structural quality. Still, the PEALD of AlN offers competitive mechanical performance and property tuning possibilities in comparison to established magnetron sputtering of AlN. Specifically, PEALD could be considered as a primary deposition method for applications leveraging PEALD's higher degree of conformality and thickness control, such as NEMS and MEMS fabrication. However, for classical flat-surface-coating purposes, the sputter deposition of AlN will dominate due to the combination of low costs and high technical performance.

ACKNOWLEDGMENTS

The authors express their gratitude to Tommi Riekkinen for deposition of the PVD samples and D. Sc. Sakari Sintonen for performing the majority of the X'Pert Pro Diffractometer based XRR and XRD analysis and providing manuscript comments. This work has been carried out within the MECHALD project funded by Tekes and is linked to the Finnish Centres of Excellence in Atomic Layer Deposition (Reference No. 251220) and Nuclear and Accelerator Based Physics (Reference Nos. 213503 and 251353) of the Academy of Finland. Micronova, the Center for Micro and Nanotechnology, is acknowledged for providing the majority of the facilities and equipment for the research. The authors acknowledge the provision of facilities by OtaNano—Nanomicroscopy Center (Aalto-NMC). Part of the results was presented at the ALD 2016 conference (Dublin, Ireland, July 24–27).

[1]S. Strite and H. Morkoç, J. Vac. Sci. Technol. B **10**, 1237 (1992).
[2]M. Lakin, IEEE Trans. Ultrason. Ferroelectr. **52**, 707 (2005).
[3]H.-C. Seo, I. Petrov, and K. Kim, J. Electron. Mater. **39**, 1146 (2010).
[4]A. V. Lobanova, E. V. Yakovlev, R. A. Talalaev, S. B. Thapa, and F. Scholz, J. Cryst. Growth **310**, 4935 (2008).
[5]S. Stevens, A. Ohtani, M. Kinniburgh, and R. Beresford, Appl. Phys. Lett. **65**, 321 (1994).
[6]F. Hasegawa, T. Takahashi, K. Kubo, and Y. Nannichi, Jpn. J. Appl. Phys. **26**, 1555 (1987).
[7]M. Broas, P. Sippola, T. Sajavaara, V. Vuorinen, A. P. Perros, H. Lipsanen, and M. Paulasto-Kröckel, J. Vac. Sci. Technol. A **34**, 041506 (2016).
[8]V. Rontu, P. Sippola, M. Broas, G. Ross, T. Sajavaara, H. Lipsanen, M. Paulasto-Kröckel, and S. Franssila, J. Vac. Sci. Technol. A **36**, 021508 (2018).
[9]Q.-P. Wei, X.-W. Zhang, D.-Y. Liu, J. Li, K.-C. Zhou, and Z.-M. Yu, Trans. Nonferr. Metal Soc. **24**, 2845 (2014).

[10]E. Iborra, J. Olivares, M. Clement, L. Vergara, A. Sanz-Hervás, and J. Sangrador, Sens. Actuators A: Phys. **115**, 501 (2004).
[11]I. C. Oliveira, K. G. Grigorov, H. S. Maciel, M. Massi, and C. Otani, Vacuum **75**, 331 (2004).
[12]H. Y. Liu, G. S. Tang, F. Zeng, and F. Pan, J. Cryst. Growth **363**, 80 (2013).
[13]J. H. Lee, W. M. Kim, T. S. Lee, M. K. Chung, B.-K. Cheong, and S. G. Kim, Surf. Coat. Technol. **133–134**, 220 (2000).
[14]R. B. Karabalin, M. H. Matheny, X. L. Feng, E. Defaÿ, G. Le Rhun, C. Marcoux, S. Hentz, P. Andreucci, and M. L. Roukes, Appl. Phys. Lett. **95**, 103111 (2009).
[15]B.-H. Hwang, C.-S. Chen, H.-Y. Lu, and T.-C. Hsu, Mater. Sci. Eng. A Struct. **325**, 380 (2002).
[16]S.-H. Lee, J.-K. Lee, and K. H. Yoon, J. Vac. Sci. Technol. A **21**, 1 (2003).
[17]H. Matsumoto, K. Asai, N. Kobayashi, S. Nagashima, A. Isobe, N. Shibagaki, and M. Hikita, Jpn. J. Appl. Phys. **43**, 8219 (2004).
[18]R. L. Puurunen, J. Appl. Phys. **97**, 121301 (2005).
[19]F. Gao, S. Arpiainen, and R. L. Puurunen, J. Vac. Sci. Technol. A **33**, 010601 (2015).
[20]R. L. Puurunen, J. Saarilahti, and H. Kattelus, ECS Trans. **11**, 3 (2007).
[21]J. Jokinen, P. Haussalo, J. Keinonen, M. Ritala, D. Riihelä, and M. Leskelä, Thin Solid Films **289**, 159 (1996).
[22]H. B. Profijt, S. E. Potts, M. C. M. van de Sanden, and W. M. M. Kessels, J. Vac. Sci. Technol. A **29**, 050801 (2011).
[23]H. Van Bui, F. B. Wiggers, A. Gupta, M. D. Nguyen, A. A. I. Aarnink, M. P. de Jong, and A. Y. Kovalgin, J. Vac. Sci. Technol. A **33**, 01A111 (2015).
[24]M. Bosund, T. Sajavaara, M. Laitinen, T. Huhtio, M. Putkonen, V.-M. Airaksinen, and H. Lipsanen, Appl. Surf. Sci. **257**, 7827 (2011).
[25]A. Pyymaki Perros, H. Hakola, T. Sajavaara, T. Huhtio, and H. Lipsanen, J. Phys. D Appl. Phys. **46**, 505502 (2013).
[26]P. Motamedi and K. Cadien, J. Cryst. Growth **421**, 45 (2015).
[27]H. Altuntas, T. Bayrak, S. Kizir, A. Haider, and N. Biyikli, Semicond. Sci. Technol. **31**, 075003 (2016).
[28]L. Kilpi, O. M. E. Ylivaara, A. Vaajajoki, J. Malm, S. Sintonen, M. Tuominen, R. L. Puurunen, and H. Ronkainen, J. Vac. Sci. Technol. A **34**, 01A124 (2016).
[29]M. Laitinen, M. Rossi, J. Julin, and T. Sajavaara, Nucl. Instrum. Methods B **337**, 55 (2014).
[30]O. M. E. Ylivaara *et al.*, Thin Solid Films **552**, 124 (2014).
[31]W. C. Oliver and G. M. Pharr, J. Mater. Res. **7**, 1564 (1992).
[32]S.-R. Jian, G.-J. Chen, and T.-C. Lin, Nanoscale Res. Lett. **5**, 935 (2010).
[33]Ioffe Institute, "New semiconductor materials, characteristics and properties," see http://www.ioffe.ru/SVA/NSM/Semicond/AlN/basic.html, accessed 7 February 2018.
[34]S. Goerke *et al.*, Appl. Surf. Sci. **338**, 35 (2015).
[35]H. B. Profijt, M. C. M. van de Sanden, and W. M. M. Kessels, J. Vac. Sci. Technol. A **31**, 01A106 (2013).
[36]ICSD, see https://icsd.fiz-karlsruhe.de/ based on H. Schulz and K. H. Thiemann, Solid State Commun. **23**, 815 (1977).
[37]X.-H. Xu, H.-S. Wu, C.-J. Zhang, and Z.-H. Jin, Thin Solid Films **388**, 62 (2001).
[38]H. Cheng, Y. Sun, J. X. Zhang, Y. B. Zhang, S. Yuan, and P. Hing, J. Cryst. Growth **254**, 46 (2003).
[39]C.-C. Cheng, Y.-C. Chen, H.-J. Wang, and W.-R. Chen, Jpn. J. Appl. Phys. **35**, 1880 (1996).
[40]M. A. Moram and M. E. Vickers, Rep. Prog. Phys. **72**, 036502 (2009).
[41]J. S. Cherng, T. Y. Chen, and C. M. Lin, Thin Solid Films **519**, 6797 (2011).
[42]M. Alevli, C. Ozgit, I. Donmez, and N. Biyikli, J. Cryst. Growth **335**, 51 (2011).
[43]D. Riihelä, M. Ritala, R. Matero, M. Leskelä, J. Jokinen, and P. Haussalo, Chem. Vapor Depos. **2**, 277 (1996).
[44]H.-Y. Shih, W.-H. Lee, W.-C. Kao, Y.-C. Chuang, R.-M. Lin, H.-C. Lin, M. Shiojiri, and M. J. Chen, Sci. Rep. **7**, 39717 (2017).
[45]L. Kilpi *et al.*, J. Vac. Sci. Technol. A **36**, 01A122 (2018).
[46]See supplementary material at https://doi.org/10.1116/1.5038856 for the PEALD AlN films crystallite size data.